551.509.314:509.5:547.5

INVESTIGATION OF THE FORECASTING ERROR OF A SIMPLE BAROTROPIC MODEL WITH THE AID OF EMPIRICAL ORTHOGONAL FUNCTIONS

PART I

by

JUHANI RINNE

Department of Meteorology,
University of Helsinki

Abstract

Empirical orthogonal functions have been determined from a sample of 48 practically independent objective 500 mb height analyses given in a grid of 1080 points. The eigenfunctions determined from the sample of the corresponding barotropic forecasts differ from those of the analysis sample more than might be expected. This is explained by a rotation in the forecast space caused by small but systematic forecasting errors. The difference between the eigenfunctions of the analysis space and the forecast space has been largely eliminated by a rotation in the forecast space. The remaining difference, »the forecasting error», shows a forecasted erroneous wave speed in agreement with the theoretical considerations, and also a false deformation of the components. In addition the boundary error has been illustrated.

The forecasts have been expanded in the eigenfunctions of the analysis space in order to filter out the erroneous non-atmospheric part of the forecasts. The reproduced forecasts then show a smaller forecasting error. In particular the boundary error has been much reduced. Because of the smallness of the samples, it is not possible to say much more about the efficiency of the presented correction method expect that it seems to work well.

1. *Introduction*

The aim of this study is an examination of and an attempt to reduce the forecasting error of a simple barotropic model with the aid of empirical orthogonal functions.

2. *The computing method*

The method used in the determination of the empirical orthogonal functions is a slight modification of that discussed by HOLMSTRÖM [3]. In our case this method was found to be time consuming. Further use of the method would first require a more thorough examination of its convergence properties. For this reason we shall in the following repeat only the principal characteristics of the functions generated by the above mentioned method.

If we have a meteorological parameter $z(t\,,i\,,j)$ depending on time (t) and on horizontal coordinates $(i\,,j)$, we may depict it by the series

$$z(t,i\,,j) - \overline{z(t\,,i\,,j)} \simeq \sum_{\nu=1}^{N} C_\nu(t) f_\nu(i\,,j) \tag{2.1}$$

where the bar refers to averaging with respect to time. In this series we have the following properties:

1) The »waves» $f_\nu(i\,,j)$ are orthogonal to each other and normalized to one, *i.e.*

$$\sum_{i,j} f_\nu(i\,,j) f_\mu(i\,,j) dA(i\,,j) = \delta_\mu^\nu\,, \tag{2.2}$$

where

$$\delta_\mu^\nu = 0\,, \quad \text{if} \quad \nu \neq \mu\,, \quad \text{and} \quad \delta_\nu^\nu = 1\,.$$

For the areal elements $dA(i\,,j)$

$$\sum_{i,j} dA(i\,,j) = 1\,. \tag{2.3}$$

2) The »amplitudes» $C_\nu(t)$ are not correlated to each other, *i.e.*

$$\sum_{t} C_\nu(t) C_\mu(t) = 0\,, \quad \text{if} \quad \nu \neq \mu\,, \tag{2.4}$$

3) The functions are final, *i.e.* $C_\nu(t) f_\nu(i\,,j)\,,\ \nu \leq N$, is independent of the number N,

4) The functions have the maximum efficiency in the representation of the quantity $z(t, i, j) - \overline{z(t, i, j)}$, where the efficiency will be measured by the variance reduction due to the functions.

3. *The data*

The analysis sample consists of the 500 mb height analyses of every 16th day 00 GMT of each month during 1965—68 (48 cases). These objective analyses have been produced by the routine program of the Swedish Meteorological and Hydrological Institute.

The forecast sample consists of the 24 hour barotropic forecasts corresponding to the verification analyses mentioned above and are thus those valid on the 16th day 00 GMT of each month (48 cases).

No use of a balance equation has been made. The forecasted quantity has been z, the height of the 500 mb surface. All of the forecasts have been slightly smoothed after the last time step.

The peculiarity of the forecasting model is that the Rossby parameter equals zero, *i.e.* $\beta \equiv 0$. This shortcircuiting has been counterbalanced by a larger Cressman correction ($q = 1.5 \times 10^{-12}$ m^{-2} instead of $q = 0.75 \times 10^{-12}$ m^{-2}), the well known semiempirical correction for the retaining of the very long waves. These modifications eliminate the retrogression effect. All waves move eastward but the longest are practically standing waves. The quality of the forecasts has been satisfactory, though the forecasts carried out with the conventional barotropic model seem to be somewhat better. Because the structure of the model is not essential for our purposes, we refer to SÖDERMAN and RINNE [5] for details.

All data have been punched for the grid presented in Fig. 1, which thereby determines the areal elements $dA(i, j)$[1].

---

1) This sounds simple, but, unfortunately, is not so easily done. An error in coding the program that computed the map scale factor, k^2, resulted in a relatively complicated version of the distribution of the factor which is close to the distribution of k. As the map projection is true at 60°N ($k = 1$), the areal elements are nearly correctly determined for 60°N, but are too small in the case of the northern latitudes and too large in the case of the southern latitudes. In other words, throughout this study the computations have been performed not on the projection plane, nor on the sphere, but on a surface between these two. This irritating error seems, however, not to have been serious.

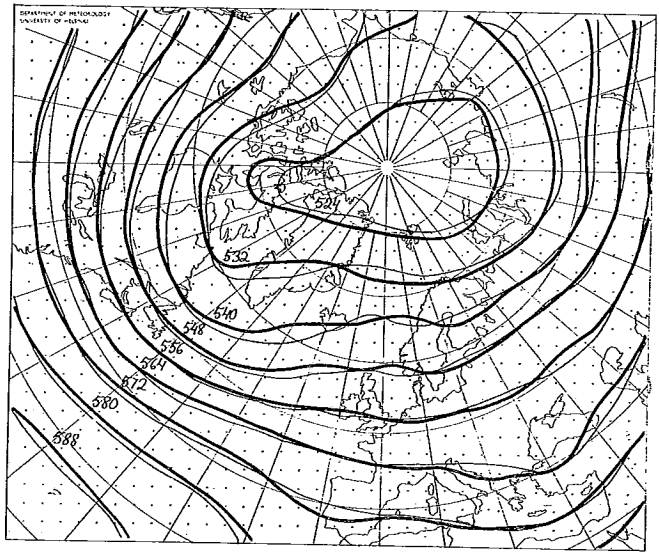

Fig. 1. The mean field of the 500 mb height analyses $\overline{z(t, i, j)}$, thick line) and that of the corresponding forecasts $\overline{z'(t, i, j)}$, thin line) in the case of 48 practically independent conditions. The map projection is a polar stereographic one, true at 60°N, where the grid interval is 300 km. The number of gridpoints is 30×36.

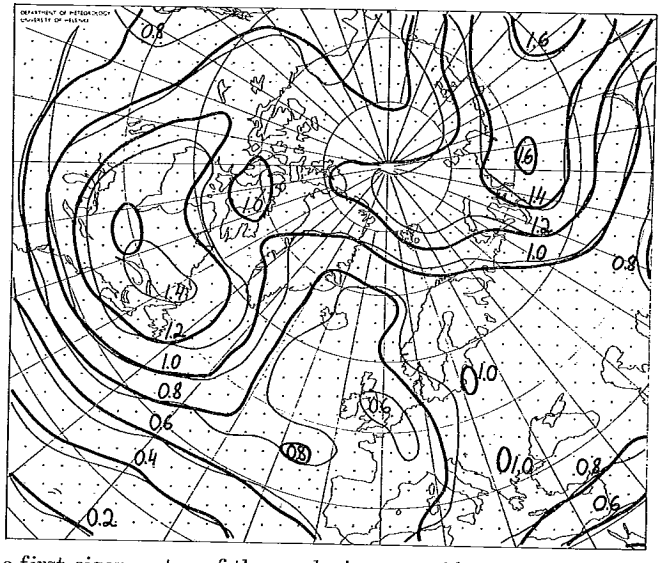

Fig. 2a. The first eigenvector of the analysis space (f_1, thick line) and that of the forecast space (f_1', thin line). The spacing corresponds to 40 gdm in the extremal case of $C_1 = 200$ gdm. The observed absolute maximum was $\max|C_1(t)| = 209$ gdm.

4. *The eigenfunctions*

The variance reduction (Table 1) and the wave pattern (Fig. 2a) of the first component of the analysis space agree with those found by CRADDOCK and FLOOD [1]. Also the general distribution of the variance reduction on the different components given in that paper is similar to that of Table 1. CRADDOCK's and FLOOD's components numbered 2, 5 and 6 (or a combination of 4 and 6) seem to have somewhat similar wave patterns to the components, 2, 4 and 3 in this study, respectively.

The significance of the components will be discussed later.

5. *Comparison between the analysis space and the forecast space*

The mean of the analyses and the mean of the forecasts do not exactly coincide at the boundaries, though the boundary assumption of the forecasting model has been $\partial z/\partial t = 0$ (Fig. 1). However, just because of this assumption, the boundary values of the forecast represent the conditions 24 hours before. Thus the boundary differences visualize the statistical error between two analysis samples due to the limited sample size. The differences in the interior of the grid are of the same order of magnitude and may thus be purely random. However, the differences appear to be systematic and hence indicate a forecasted eastward motion of the standing waves. For instance, the main Canadian through, the ridge over Greenland, and the eastern Mediterranean through have moved eastward.

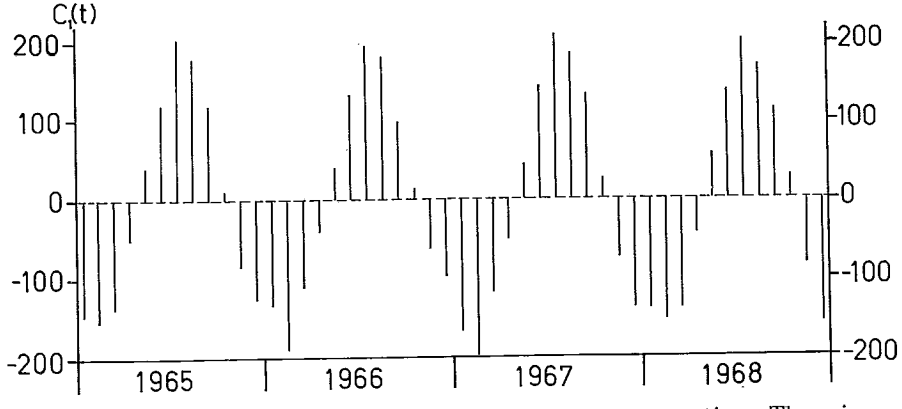

Fig. 2b. The amplitude of the first component, $C_1(t)$, versus time. There is one observation for every 16th day of each month during 1965—1968 (48 cases). Unit: gdm.

Table 1. The variance reduction of the empirical orthogonal functions. The samples consist of 48 practically independent analyses and the corresponding 500 mb barotropic 24 hour forecasts.

Component number	Variance reduction of the components					
	of the analysis space			of the forecast space		
	Value in gdm²	Per cent	Per cent Cum	Value in gdm²	Per cent	Per cent Cum
1	16725	58.9	58.9	16593	58.8	58.8
2	1533	5.4	64.3	1435	5.1	63.9
3	1365	4.8	69.1	1398	5.0	68.9
4	1078	3.8	72.9	1008	3.6	72.5
5	922	3.2	76.1	898	3.2	75.7
6	839	3.0	79.1	882	3.1	78.8
7	624	2.2	81.2	726	2.6	81.4
8	582	2.1	83.3	641	2.3	83.6
9	544	1.9	85.2	524	1.9	85.5
10	462	1.6	86.8	485	1.7	87.2
11	444	1.6	88.4	431	1.5	88.7
12	357	1.3	89.7	328	1.2	89.9
13	314	1.1	90.8	314	1.1	91.0
14	287	1.0	91.8	281	1.0	92.0
15	248	0.9	92.7	247	0.9	92.9
16	231	0.8	93.5	239	0.9	93.7
17	198	0.7	94.2	192	0.7	94.4
18	182	0.6	94.8			
19	145	0.5	95.3			
20	132	0.5	95.8			
21	123	0.4	96.2			
22	113	0.4	96.6			
23	101	0.4	97.0			
24	94	0.3	97.3			
25	84	0.3	97.6			
26	74	0.3	97.8			
27	61	0.2	98.1			
28	57	0.2	98.3			
29	54	0.2	98.4			
30	48	0.2	98.6			
31	42	0.1	98.8			
32	42	0.1	98.9			
33	36	0.1	99.0			
residual	273	1.0	100.0	1576	5.6	100.0
Total var.	28410			28198		

We can observe a similar erroneous eastward motion of the standing climatological waves in the patterns of the first components also (Fig. 2a).

At first glance it would seem to be difficult to explain the remarkable differences between the second and third components of the analysis and the forecast space, as these components should be statistically significant (Figs. 3 and 4). Because the variances of the amplitudes of these components are adjacent, it is possible that the waves (*e.g.* $\sin \Phi$, $\cos \Phi$) of the analysis space have in the forecast space been represented by the same components with an additional phase shift ($\sin (\Phi - \Phi_0)$, $\cos (\Phi - \Phi_0)$). Figs. 3 and 4 do not show any distinct phase shift between the analysis and forecast components, but the rotation in the forecast space may be very complicated.

Let the equation

$$z(t\,,i\,,j) - \overline{z(t\,,i\,,j)} = \sum_{\nu} C_{\nu}(t) f_{\nu}(i\,,j) \tag{5.1}$$

and the equation

$$z'(t\,,i\,,j) - \overline{z'(t\,,i\,,j)} = \sum_{\nu} C'_{\nu}(t) f'_{\nu}(i\,,j) \tag{5.2}$$

represent the conditions in the analysis and forecast spaces, respectively. The rotated vectors

$$f''_{\mu}(i\,,j) = \sum_{\nu=1}^{14} a_{\mu\nu} f'_{\nu}(i\,,j)\,, \quad \mu \text{ small enough,}$$

where

$$a_{\mu\nu} = \sum_{i,j} f_{\mu}(i\,,j)\, f'_{\nu}(i\,,j) dA(i\,,j)\,, \tag{5.3}$$

form a *nearly* orthogonal basis and even such that

$$\sum_{i,j} (f''_{\mu} - f_{\mu})\, f'_{\nu}\, dA \simeq 0\,, \quad \nu \leq 14\,,$$

i.e., it is impossible to depict the difference $f''_{\mu} - f_{\mu}$ with the aid of the first 14 components of the forecast space. In other words, it is nearly impossible to perform a rotation in the forecast space which would make the vectors f''_{μ} and f_{μ} lie closer to each other. Thus the difference $f''_{\mu} - f_{\mu}$ may be used to illustrate the forecasting error associated with the component f_{μ}, when μ is small enough.

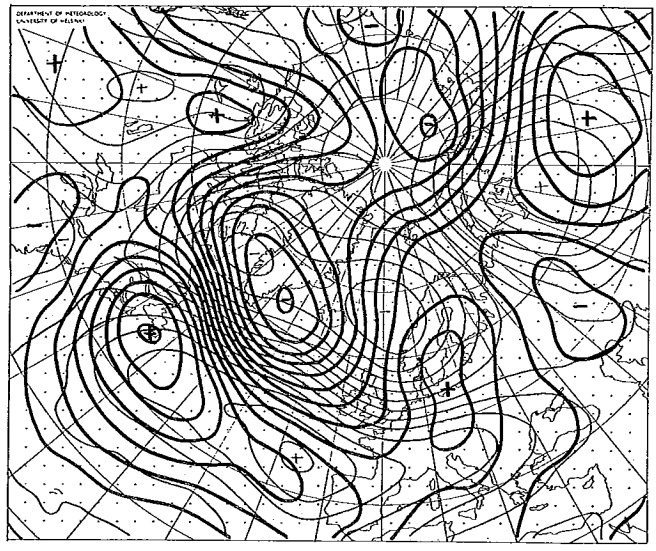

Fig. 3. As Fig. 2a, but showing the second eigenvectors, with $\max_t |C_2(t)| = 97$ gdm, and the spacing corresponding to 40 gdm in the extremal case of $C_2 = 100$ gdm.

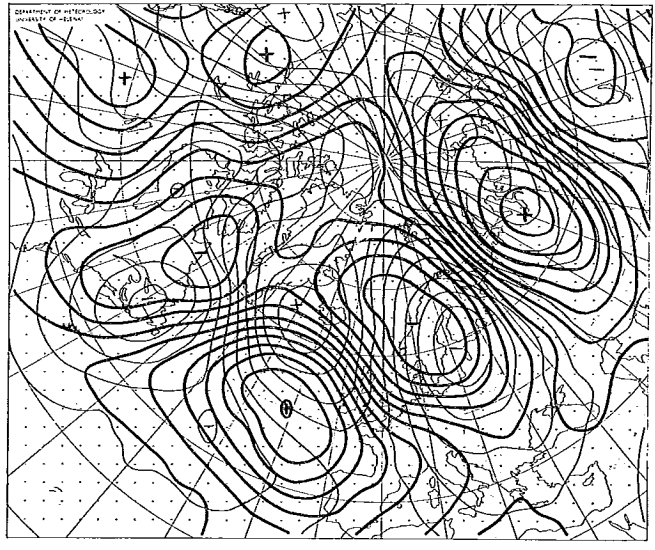

Fig. 4. As Fig. 3, but showing the third eigenvectors; $\max_t |C_3(t)| = 80$ gdm.

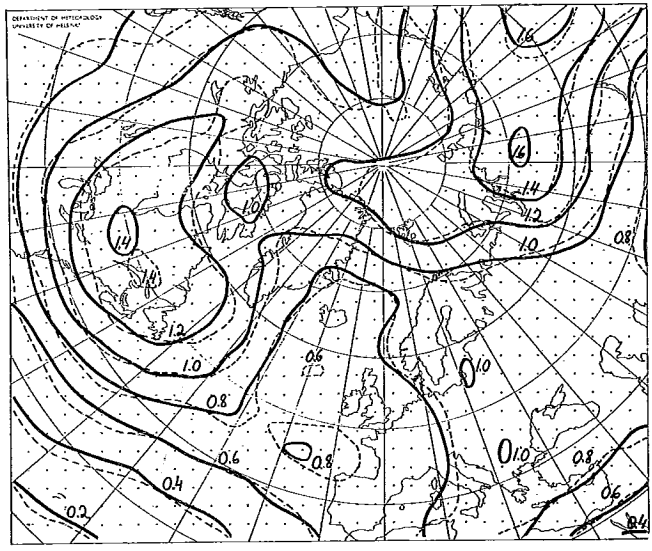

Fig. 5. The first eigenvector of the analysis space (f_1, solid line) and the corree sponding eigenvector of the rotated forecast space (f_1^*, broken line). The spacing corresponds to 40 gdm in the extremal case of $C_1 = 200$ gdm. The observed absolute maximum was $\max_t |C_1(t)| = 209$ gdm.

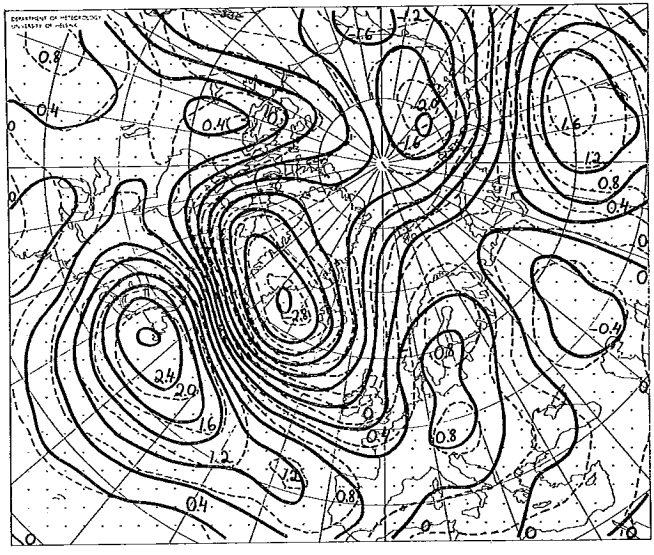

Fig. 6. As Fig. 5 but for the second eigenvectors; $\max_t |C_2(t)| = 97$ gdm. Th- spacing corresponds to 40 gdm in the extremal case of $C_2 = 100$ gdm.

The rotated first component shows erroneous eastward movements similarly to the non-rotated one, but less pronounced. As both of these components are obviously statistically significant, there should be an explanation of this difference. Perhaps we could interpret it by saying that Fig. 2a tends to show the error with an yearly oscillation, while Fig. 5 tends to show only the error associated with the first component.

Because the samples used are small and the performed rotation is not complete, one has to be careful when examining the rotated components. In spite of this, we may perhaps state that, in addition to the first component, even the other rotated components, in comparison with the analysis components, show a similar, more or less regular, erroneous eastward motion. We also observe a false deformation of the rotated wave patterns, and note the boundary effect on the upper boundary in Fig. 9 and on the left boundary in Fig. 10. In the latter case there exists a center that has been kept fixed by the forecasting model, while in analyses it has moved towards the northeast.

As the forecast space and the analysis space are very close to each other, there exists an orthogonal basis in the analysis space such that the second and third components resemble the corresponding components of the forecast space. For instance, if one is interested in examining the zonal index over the Atlantic, the forecast components would perhaps be more suitable than the presented analysis components, as f_2' shows a zonal flow, while f_3' has a more cellular structure. The problem is thus not only to find the orthogonal functions but also to rotate them in the most suitable way.

6. *The forecasting error*

The forecasting error will be defined as the mean square deviation

$$E = \overline{\sum_{i,j} \{ \sum_{\nu} C_\nu(t) f_\nu(i\,,j) - \sum_{\nu} C_\nu'(t) f_\nu'(i\,,j) \}^2 dA(i\,,j)}\,. \tag{6.1}$$

We reproduce the forecasts $\sum_{\nu} C_\nu'(t) f_\nu'(i\,,j)$ by replacing the components f_ν' by their estimates in the analysis space, *i.e.* by the estimates

$$f_\nu'(i\,,j) \simeq \sum_{\mu}^{n_\nu} a_{\mu\nu} f_\mu(i\,,j)\,, \tag{6.2}$$

where the coefficients $a_{\mu\nu}$ are given by (5.3). Then the remaining error will be

$$E_r = \sum_{i,j} \{ \sum_{\nu} C_\nu(t) f_\nu(i\,,j) - \sum_{\nu} C'_\nu(t) \sum_{\mu}^{n_\nu} a_{\mu\nu} f_\mu\,(i\,,j)\}^2\, dA(i\,,j)\,,$$

while the removed part of the error is given by $E - E_r$. From the orthogonality properties it follows that

$$E_r = \overline{\sum_{\nu} \{C_\nu(t) - \sum_{\mu}^{n_\nu} a_{\nu\mu}\, C'_\mu(t)\}^2}\,. \tag{6.3}$$

We must now truncate the series (6.2) in such a way that (6.3) will be minimized. However, up to $\mu = 17$ there were no significant indications of such truncation points n_ν. Therefore it was decided to use non-truncated series.

If

$$D_\nu(t) = \sum_{i,j} \{z'(t\,,i\,,j) - \overline{z'(t\,,i\,,j)}\} f_\nu(i\,,j) dA(i\,,j)\,,$$

which from (5.2) becomes

$$D_\nu(t) = \sum_{\mu} a_{\nu\mu}\, C'_\mu(t)\,,$$

then for the non-truncated series we have

$$E_r = \overline{\sum_{\nu} \{C_\nu - D_\nu\}^2}\,. \tag{6.4}$$

Evidently we may refer to $E_{r\nu} = \overline{(C_\nu - D_\nu)^2}$ as the remaining error associated with the ν^{th} component of the analysis space.

According to Table 2 there are no components with a pronounced large or small error variance expect perhaps the first component. Obviously the distribution of the removed error (*cf.* Figs. 5—10) on different components has also been smooth.

Because the components $\nu > 33$ were not determined, we had to put $D_\nu \equiv 0$ when $\nu > 33$. However, this seems to be a disadvantageous approximation, as the correlation between the predictands C_ν and the corresponding predictors D_ν seems to differ from zero even when $\nu > 33$ (Fig. 16). Therefore we evaluate

$$\overline{\sum_{\nu=34} (C_\nu - D_\nu)^2} \simeq \overline{0.7 \sum_{\nu=34} C_\nu^2}\,,$$

where the coefficient 0.7 is an estimated factor which should perhaps be higher. In this way the remaining error variance would be 2104 gdm^2,

Table 2. The variance of the remaining error associated with the ν^{th} component of the analysis space. Unit: gdm².

Component ν	Remainding error variance $E_{r\nu}$
1	59
2	119
3	95
4	101
5	112
6	82
7	65
8	91
9	88
10	73
11	111
12	72
13	52
14	38
15	65
16	52
17	58
18	76
19	50
20	45
21	23
22	42
23	31
24	49
25	41
26	40
27	39
28	25
29	27
30	21
31	18
32	24
33	26
> 33	273 (if $D_\nu \equiv 0$, when $\nu > 33$)
Sum	2185

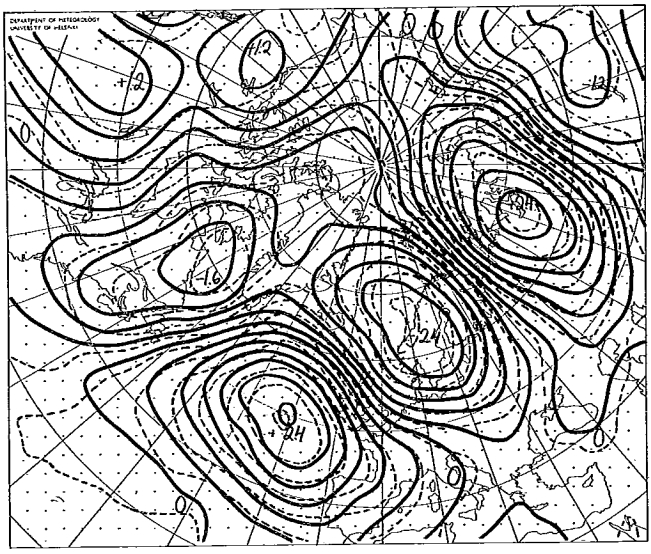

Fig. 7. As Fig. 6 but for the third eigenvectors; $\max_t |C_3(t)| = 80$ gdm.

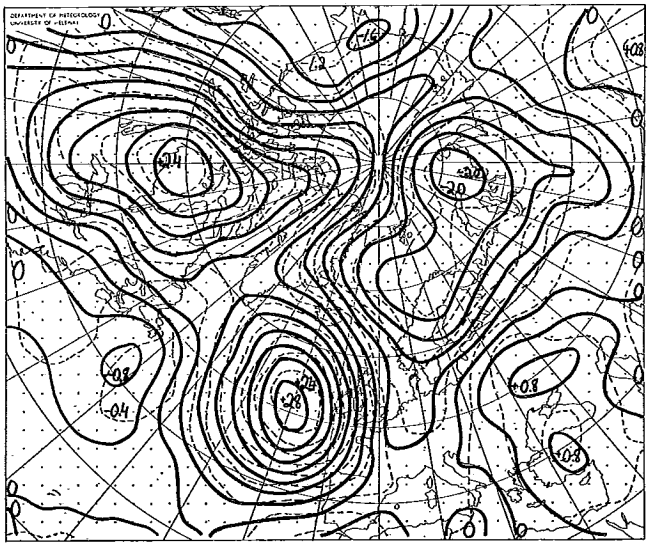

Fig. 8. As Fig. 6 but for the fourth eigenvectors; $\max_t |C_4(t)| = 78$ gdm.

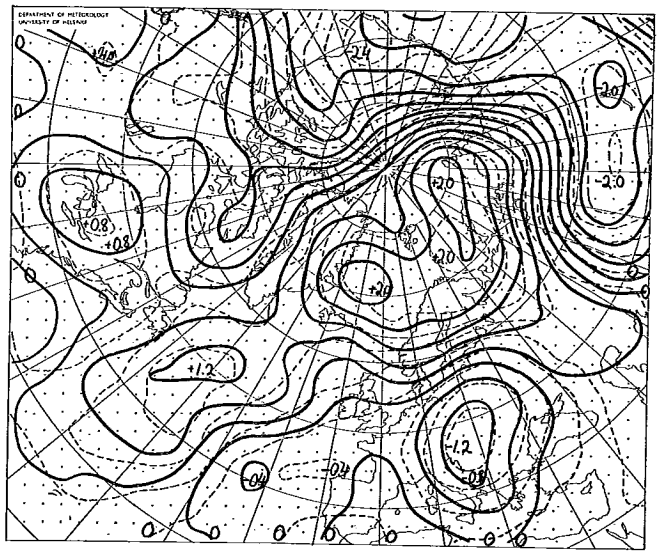

Fig. 9. As Fig. 6, but for the 5th eigenvectors; $\max_t |C_5(t)| = 85$ gdm.

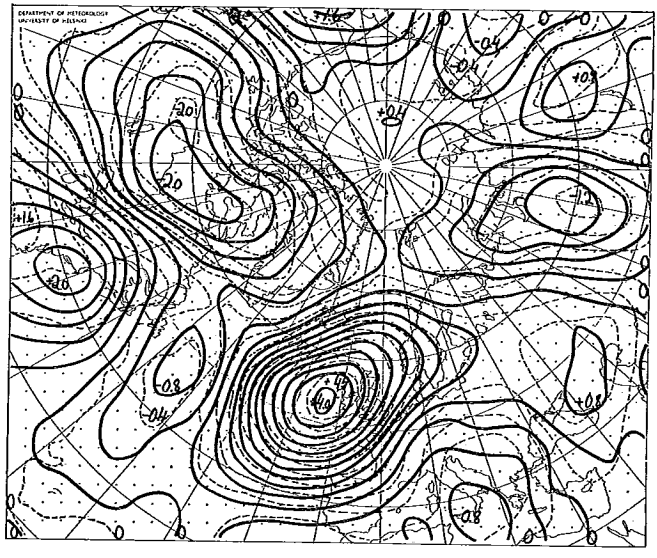

Fig. 10. As Fig. 6, but for the 6th eigenvectors; $\max_t |C_6(t)| = 68$ gdm.

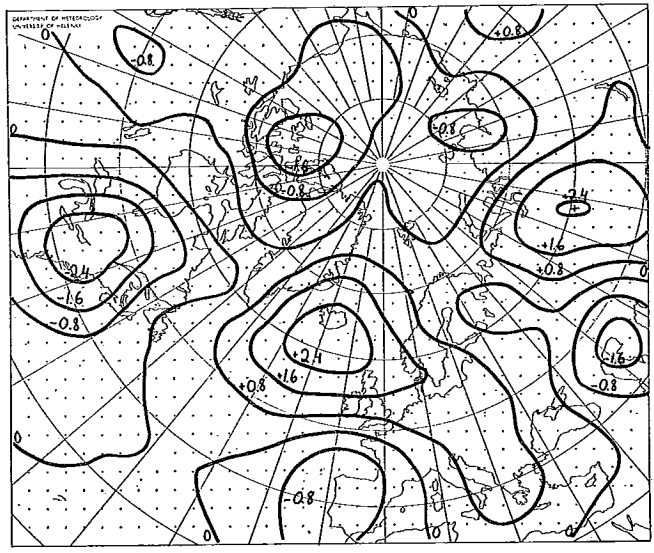

Fig. 11. The 11th eigenvector of the analysis space illustrating a less predictable component. The spacing corresponds to 40 gdm in the extremal case of $C_{11} = 50$ gdm. The observed absolute maximum was $\max_t |C_{11}(t)| = 71$ gdm.

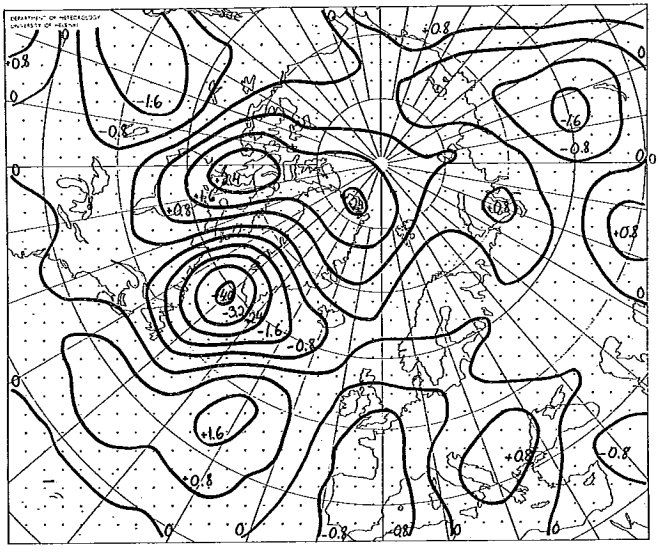

Fig. 12. The 14th eigenvector of the analysis space illustrating a more predictable component. The spacing corresponds to 40 gdm in the extremal case of $C_{14} = 50$ gdm. The observed absolute maximum was $\max_t |C_{14}(t)| = 43$ gdm.

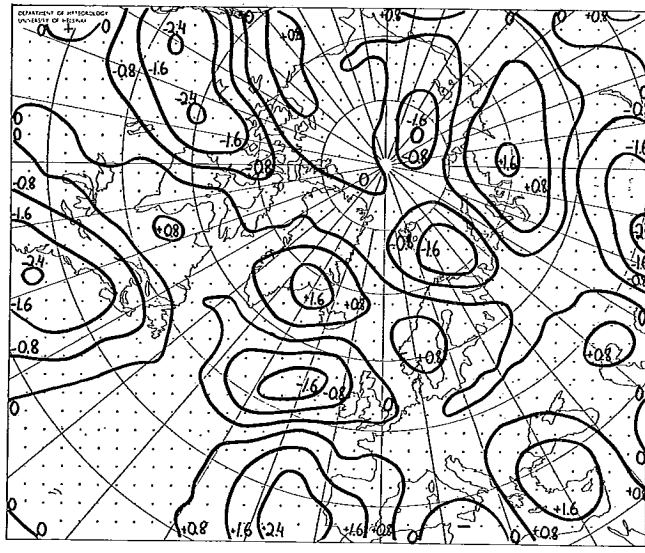

Fig. 13. As Fig. 12, but for the 18th eigenvector illustrating a less predictable component, for which max $|C_{18}(t)| = 50$ gdm.

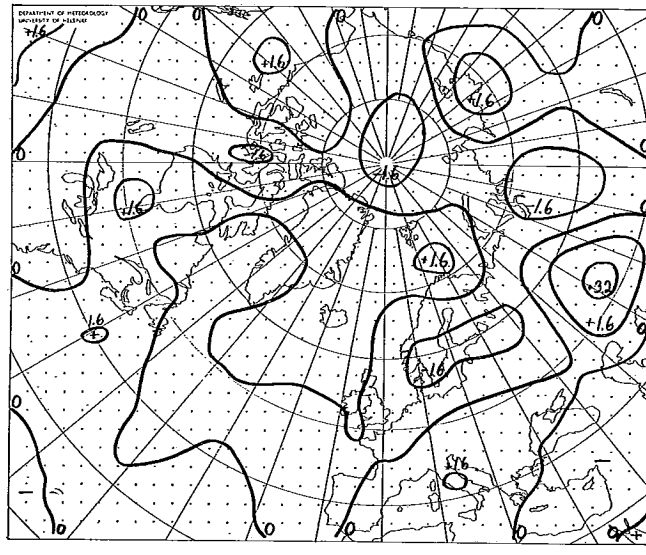

Fig. 14. The 21st eigenvector of the analysis space illustrating a more predictable component. The spacing corresponds to 40 gdm in the extremal case of $C_{21} = 25$ gdm. The observed absolute maximum was max $|C_{21}(t)| = 24$ gdm.

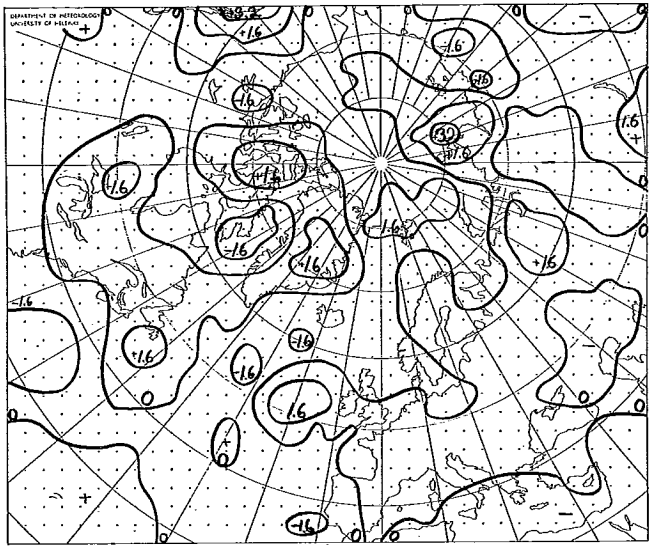

Fig. 15. As Fig. 14 but for the 33$^{\text{th}}$ eigenvector, for which $\max_t |C_{33}(t)| = 16$ gdm.

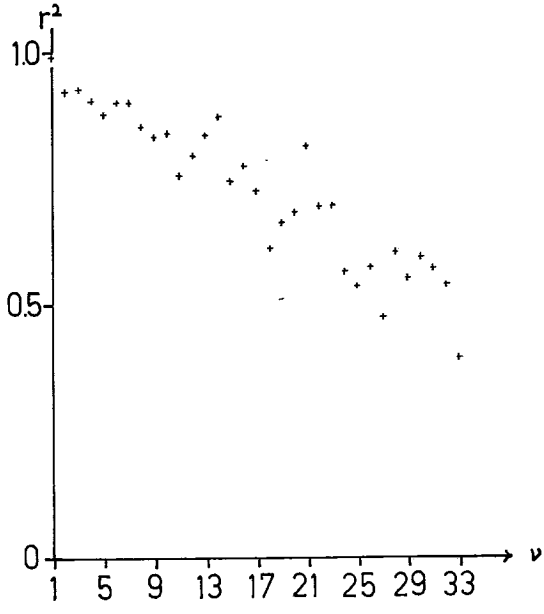

Fig. 16. The square correlation coefficient between the observed, C_ν, and the predicted, D_ν, amplitude of the ν^{th} component.

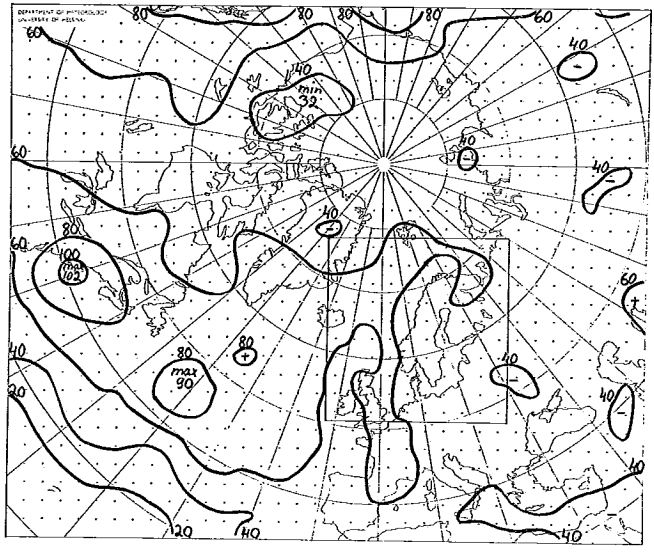

Fig. 17. The initial distribution of the r.m.s. error of 24 hour barotropic forecasts of the 500 mb height (48 cases). Unit: gdm.

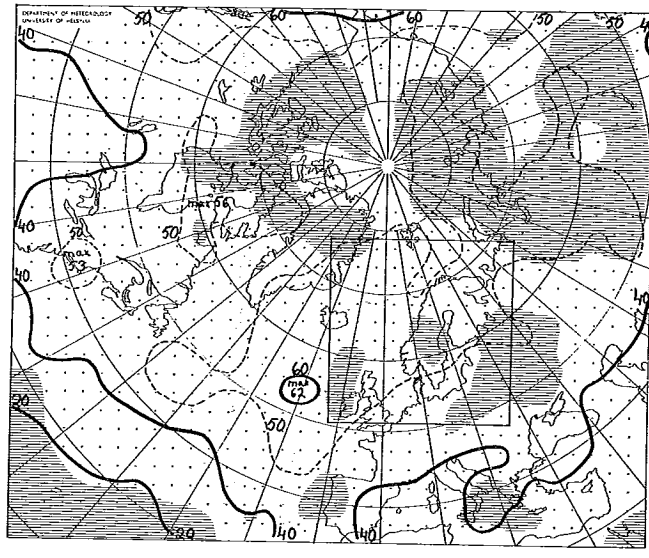

Fig. 18. The r.m.s. error of the reproduced forecasts. Over the hatched area the correction method has increased the r.m.s. error. The smaller grid shows the routine verification area. Unit: gdm.

whereas the initial error variance $\overline{\sum_{i,j} \{(z - \bar{z}) - (z' - \bar{z}')\}^2 dA}$ has been 2974 gdm². Thus in the case studied the described method has been capable of reducing the total error variance by an amount 900 gdm² or 30%. As the forecasts should be reproduced by adding $\sum_{\nu} D_\nu f_\nu$ not to $\bar{z}'$ but to $\bar{z}$, one should take into account the reduction of the forecasting error in the mean fields. In this way, the initial error variance $\overline{\sum_{i,j}(z - z')^2 dA}$ was 3091 gdm² and the reduction amounts would be 1000 gdm² or 30%. The areal distribution of the remaining r.m.s.e.,

$$\sqrt{\overline{\sum_{\nu}^{33} \{(C_\nu - D_\nu) f_\nu(i\,,j)\}^2 + 0.7\,\{z(t\,,i\,,j) - \overline{z(t\,,i\,,j)} - \sum_{\nu}^{33} C_\nu f_\nu(i\,,j)\}^2}}$$

is presented in Fig. 18.

Because we have tried to minimize the total error variance, it is natural that the areal distribution of the remaining error is smoother than and lacks the distinct extremes of the initial error field. Because the boundary error no longer dominates, the error is more geographically distributed with isolines following the latitudes. As the southern part of the Atlantic lacks observations, it is impossible to decide if the increase in error over this area is true. The increase in error over Russia is not disadvantageous, as this area is situated downstream from the verification area, which is shown by the smaller grid in Fig. 18. On the verification area the reduction of the error variance has been about 25%.

According to Fig. 16 some of the components have been more or less predictable when compared with adjacent components. Obviously the boundary error plays a role here. For instance, the less predictable components $\nu = 11$ and $\nu = 18$ have relative extremes at the inflow boundaries, whereas the more predictable components $\nu = 14$ and $\nu = 21$ show weak evidence of this kind of centers (Figs. 11—14).

Two cases of forecasts are presented in Figs. 19 and 20. Both cases have in the routine forecasts been disturbed by the boundary assumption at the inflow boundary. Otherwise the forecasts differ, the latter being one of the best, whereas the former resulted in a very low correlation coefficient in the routine verification, because the rapid development over the Eastern Atlantic was not forecasted. This error has not been corrected in the reproduced forecast, but at the boundary we may observe a satisfactory change caused by the reproduction. A similar boundary error correction has occurred also in the latter case.

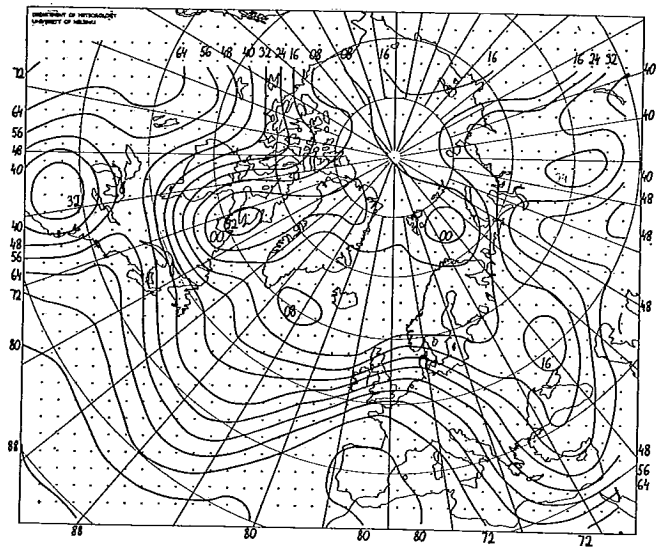

Fig. 19a. The objective analysis, Jan. 15, 1968, 00 GMT (500 mb).

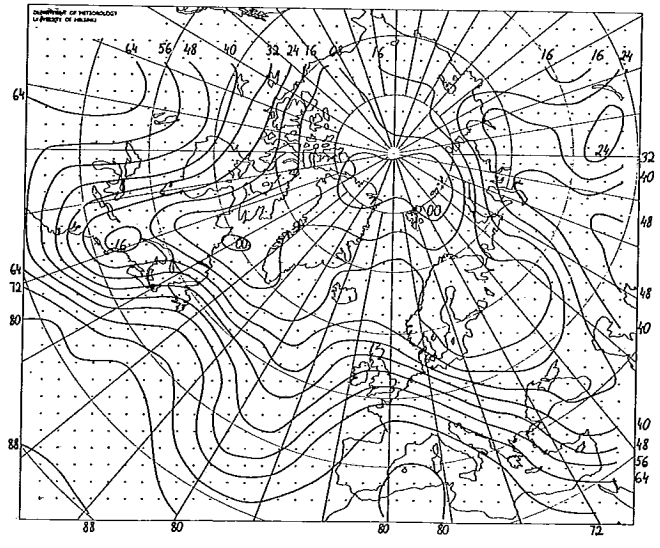

Fig. 19b. The objective analysis, Jan. 16, 1968, 00 GMT.

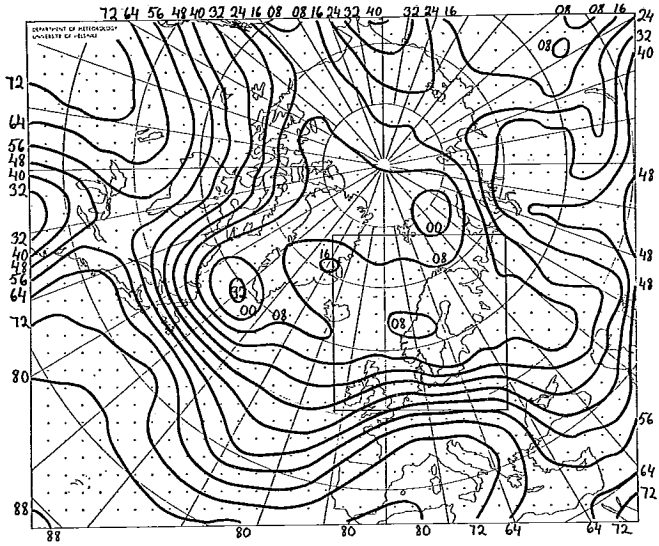

Fig. 19c. The routine 24 hour barotropic forecast, valid on Jan. 16, 1968, 00 GMT.

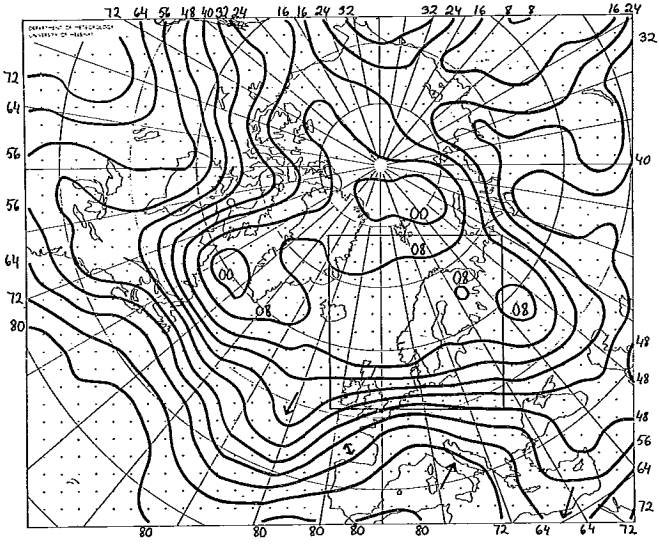

Fig. 19d. The reproduced forecast corresponding to that in Fig. 19c.

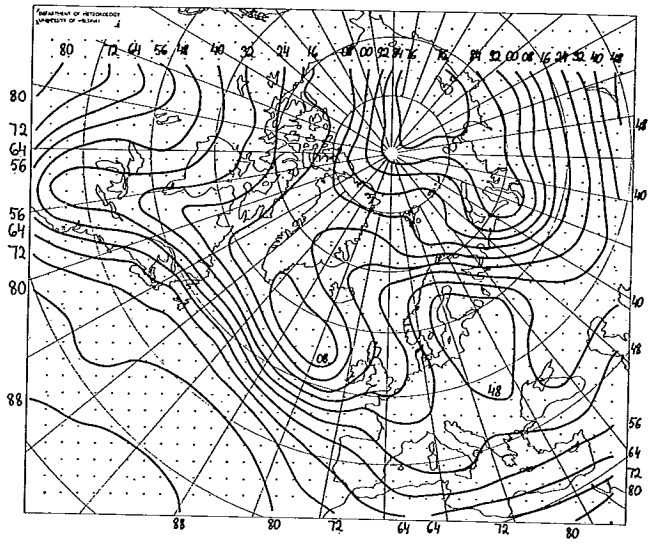

Fig. 20a. The objective analysis, Dec. 15, 1968, 00 GMT (500 mb).

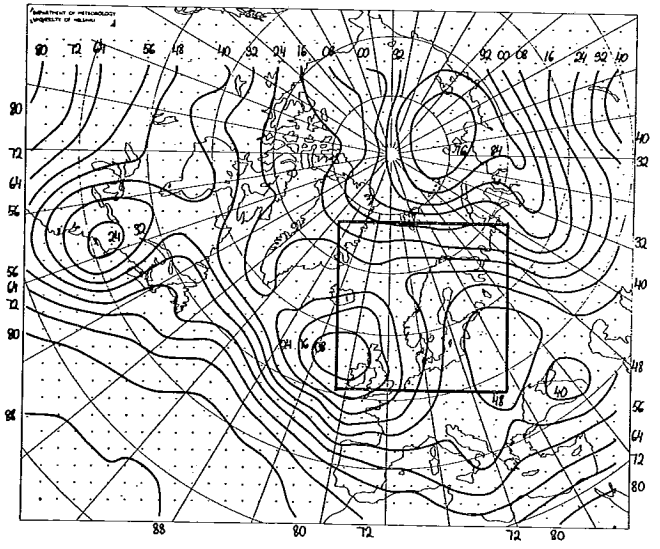

Fig. 20b. The objective analysis, Dec. 16, 1968, 00 GMT.

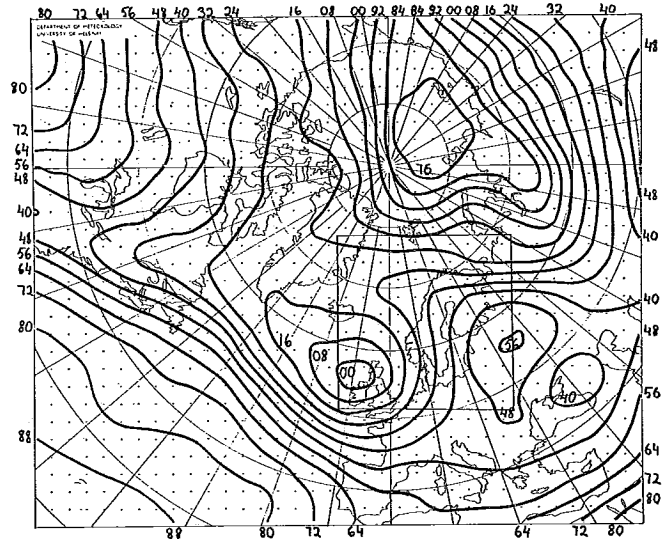

Fig. 20c. The routine 24 hour barotropic forecast, valid on Jan. 16, 1968, 00 GMT.

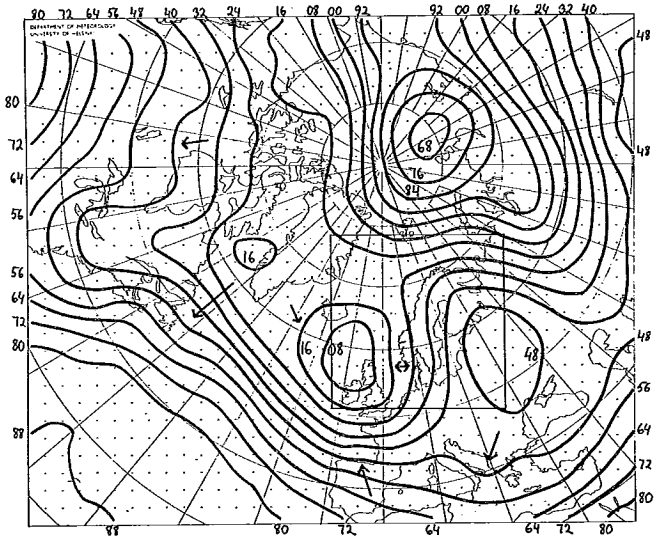

Fig. 20d. The reproduced forecast corresponding to that in Fig. 20c.

Although the smallness of our sample does not justify a discussion of the changes on the smaller scale, some interesting details are indicated by arrows in Figs. 19d and 20d.

The first ten amplitudes $C_\nu(t)$ in these two cases were (unit: gdm)

	1	2	3	4	5	6	7	8	9	10
Jan. 16, 1968	−137	25	53	−15	−14	−64	6	−71	1	0
Dec. 6, 1968	−157	61	−51	48	−20	−68	−9	31	38	−17

Note the high amplitudes of the sixth component, which indicates a center locating on the left boundary of the grid.

7. *The significance of the results*

Before examining the significance of the results, the author wishes to repeat briefly the principle of the presented correction method. The eigenfunctions have first been determined from an analysis sample, then the forecasts have been presented with the aid of these components. This is a natural way to correct the forecasts, as that part of them which is difficult to depict by the eigenfunctions of the analyses evidently does not represent any atmospheric phenomenon and thus should be eliminated.

It may appear strange that a large number of eigenfunctions have been determined from a small sample, though only the first few of them can be significant (*cf.* ЯКОВЛЕВА *et al.* [6]). However, in the conventional sense we consider the eigenfunctions to be significant, if they would be similar when determined from two independent and large samples. This concept of the significance is in our case statistically too pure for the following reasons. Firstly, as we have seen, a small but systematic difference (the forecasting error) between two samples may result in large unnatural differences in the eigenfunctions. This simply is caused by the fact that in the atmosphere the variances of the adjacent components are close to each other rather than because of a remarkable difference between the samples. Secondly, it was pointed out in Ch. 5 that, although we have statistically significant eigenfunctions, they still do not necessarily form the best basis for a particular study. Finally, it must be borne in mind that our method requires not »significant» eigenfunctions but a powerful capacity to represent the atmospheric phenomena to be predicted and to filter them out from a forecast.

Hence the requirement of the significance has in our case been reduced to that of the capacity of representation of the atmospheric phenomena. There surely exist some 500 mb phenomena which are lacking in our sample. In this sense our analysis sample has been too limited. We should therefore have more data to generate more components so as to yield the full capacity in representation. Because the efficiency in representation of the forecasting error obviously increases simultaneously, the capacity of the components to filter out the noise of the forecasts might decrease. Therefore the actual values of the error reduction have perhaps in our case been overestimated.

CRADDOCK and FLOOD (*op.cit.*) answered the question »How many eigenvectors» by concluding that »We can say that at least 25 eigenvectors should be used for most purposes while 50 will generally be too many, but between these limits the point of truncation is a matter of judgment». Therefore, in the case of our smaller area, the number of useful components is perhaps not more than 45. On the other hand, our 33 components consist of predictable, mostly large scale waves with amplitudes generally differing from zero. The wavelength of the last component ($\nu = 33$) is still about 3000 kms. Only the amplitudes of the highest components ($\nu \gtrsim 30$) tend to be zero except in a few cases. Thus nearly all of our 33 components should be representative and, when rotated in a suitable way, they should be found among the mentioned 45 »significant» components.

In the case of a regression model, where orthogonal empirical functions appear as predictors, one has to test the efficiency of the model by an independent sample of the forecasts (*cf.* LORENZ [4]). In the present case such a test sample is of minor importance, as the derived correction method does not include any statistical parameter like the regression coefficient. In fact, the present method is completely independent of the forecasting model and its errors.

Because the used analyses have been objective, they might to some extent be correlated with forecasts. It is also possible that they may have been smoothed too much. These disadvantages are not very important when compared with the influence of the limited sample size.

There is still one question to be answered, namely, whether the large error reduction in the case studied has been caused by the existence of special kinds of errors, the boundary error and the erroneous eastward motion of the long waves. It is obvious that, if there were no sources for the boundary error, the forecasting error and the error reduction would

be much smaller. However, the boundary error serves in this connection as an easily observable systematic phenomenon that does not appear in the atmosphere. On the other hand, the eastward motion of the waves is a feature typical of the atmosphere and thus the erroneous eastward movement of the waves is an easily observable phenomenon corresponding rather to the behaviour of the atmosphere. It is possible that the correction method partly interprets the latter type of error as a rotation (phase shift) in the forecast space and hence cannot satisfactorily identify the »true» and »false» atmospheres. Our special kinds of errors thus illustrate the ability of the present method rather to correct errors of very different origins. Obviously the method has also reduced errors which are not so easy to observe and not so dominating. We note in this connection that even the more complicated modern models may generate errors that are systematic and easily observable (*cf.* FAWCETT [2]).

We conclude that the analysis sample has been too small to produce eigenfunctions describing all the 500 mb phenomena to be predicted. Also, the high error reduction which has been reached is partly due to special conditions. For these reasons it is not possible to draw concrete conclusions about the validity of the presented correction method. However, the method is natural, simple in principle, and it also seems to work well, perhaps even in the case of a more complicated model.

8. *Further possibilities for reducing the error variance*

The correction method has been applied after the last time step of a forecast. It is clear that the method would have been more effective if it had been applied also earlier in the computing procedure, perhaps after every time step. For instance, the 48 hour forecasts based on the corrected 24 hours forecasts would surely be better than those based on the corresponding routine forecasts.

The areal error distribution shows that the method works overall the field considered and thus decreases the error also over areas which are not of interest. This could be avoided by modifying the areal weights suitably. For instance, the increase in error at the northern latitudes (Fig. 18) has possibly been partly caused by the false areal weighting (*cf.* Ch. 3, footnote).

So far we have determined only one statistical parameter in addition to the mean fields and the eigenfunctions, namely the truncation point of the reproduced forecasts $\sum_{\nu} D_\nu f_\nu$. This point seemed to occur some-

where after the point $\nu = 33$. One further possibility is to try to reduce the tendency of the D'_νs to be overestimates of the C'_νs (not shown here). This has been done in the present work by determining only two additional parameters and by using the values $D_\nu - 0.008\,(\nu - 2.5)\,D_\nu$ instead of the D'_νs. This crude correction resulted in a reduction of the error variance by 68 gdm^2, whereas the reduction of the more complicated scheme was not more than 100 gdm^2. The reduction is significant but not remarkable when compared with that caused by the main correction method.

The best ten regression schemes

$$C_\nu \simeq D_\nu + \sum_\mu \beta_{\mu\nu} D_\mu\,, \quad \nu = 1\,, 2\,, \ldots\,, 10\,,$$

where all of the significant (in the sense of the regression analysis) predictors D_μ were accepted, resulted in an error reduction of 335 gdm^2 or about 30 gdm^2 per component. If only one predictor had been accepted in each of the ten regression models, the corresponding reduction values would have been 115 gdm^2 or 10 gdm^2 per component. It thus seems to be possible to reduce the error with the aid of this kind of regression scheme, but conclusive verification of this would require more data. An interesting detail is that the amplitude C_2 had no significant predictors (hence $C_2 \simeq D_2$), while the amplitude estimate D_2 was a good predictor for the predictands C_3, C_4, C_5 and C_8.

As the forecasting model includes no processes generating an yearly oscillation, the forecasted amplitude of the first component should be close to that of the initial condition. To verify this the first harmonics of the amplitudes C_1 and D_1 were determined and found to be

$$C_1 \simeq -\,180.7 \cos\left(\frac{t - 26.5}{360}\,2\pi\right)$$

and

$$D_1 \simeq -\,179.4 \cos\left(\frac{t - 27.5}{360}\,2\pi\right),$$

where t is given in days. There is an obvious phase shift of about 24 hours. Since the correction of the difference between the first harmonics would reduce the error variance by 5 gdm^2, this is of minor importance.

9. *Conclusions*

Empirical orthogonal functions have been determined from a sample of 48 practically independent objective analyses. The eigenfunctions determined from the sample of the corresponding barotropic forecasts differ from those of the analysis sample more than could be expected. This is explained by a rotation in the forecast space brought about by small but more or less systematic forecasting errors. The difference between the eigenfunctions of the analysis space and the forecast space has been largely eliminated by a rotation in the forecast space. The remaining difference, »the forecasting error», shows a forecasted erroneous wave speed, in agreement with the theoretical considerations, and also a false deformation of the components. Furthermore the boundary error is illustrated.

The forecasts have been expanded in the eigenfunctions of the analysis space in order to filter out the erroneous non-atmospheric part of the forecasts. The reproduced forecasts then show a smaller forecasting error. In particular the boundary error has been much reduced. Because of the smallness of the samples, it is not possible to say more about the efficiency of the presented correction method except that it seems to work well.

Acknowledgments: The initial analyses used in this study have been obtained from the Swedish Meteorological and Hydrological Institute. Based on these analyses the barotropic forecasts have been prepared by a working group at the Department of Meteorology, University of Helsinki. The supervisor of this group was prof. L. A. Vuorela with Mr. D. Söderman as senior scientist and Mr. J. Helminen and the author as associate scientists. Miss Tuulikki Pitkänen has assisted in preparing the material for publication. She has also drawn the figures.

The working group received financial support from Valtion Luonnontieteellinen toimikunta (The National Research Council For Science). This study in particular has been supported by the Sohlberg Foundation of the Finnish Society of Sciences.

Finally the author wishes to acknowledge with appreciation helpful discussions with prof. Eero Holopainen.

REFERENCES

1. CRADDOCK, J. M. and C. R. FLOOD, 1969: Eigenvectors for representing the 500 mb geopotential surface over the Northern Hemisphere. *Quart. J. roy. Meteor. Soc.*, **95**, 576—593.
2. FAWCETT, E. B., 1969: Systematic errors in operational baroclinic prognoses at the National Meteorological Center. *Mon. Weath. Rew.*, **97**, 670—682.
3. HOLMSTRÖM, I., 1963: On a method for parametric representation of the state of the atmosphere. *Tellus*, **15**, 127—149.
4. LORENTZ, E. N., 1956: Empirical orthogonal functions and statistical weather prediction. *Sci. Rept. No. 1, Statistical Forecasting Project, Dept. of Meteorology, MIT*, Cambridge, Mass.
5. SÖDERMAN, D. and J. RINNE, 1968: Numerical weather prediction in Finland during 1967, *Progress Report*, Helsinki.
6. ЯКОВЛЕВА, Н. И., А.В. МЕЩЕРСКАЯ, Г. Д. КУДАШКИН, 1964: Исследование полей давления (геопотенциала) методом разложения по естественным составляющим. Тр. ГГО, **165**, 78—103.